MAGNETOHYDRODYNAMIC TURBULENCE PRODUCED BY RECONNECTION INSTABILITY

Marco Onofri
Dipartimento di Fisica,
Università della Calabria,
via P. Bucci, 87036 Rende (CS), Italy

Leonardo Primavera
Dipartimento di Fisica,
Università della Calabria,
via P. Bucci, 87036 Rende (CS), Italy

Pierluigi Veltri
Dipartimento di Fisica,
Università della Calabria,
via P. Bucci, 87036 Rende (CS), Italy

Francesco Malara
Dipartimento di Fisica,
Università della Calabria,
via P. Bucci, 87036 Rende (CS), Italy

ABSTRACT

We present numerical simulations of incompressible magnetohydrodynamics for the study of the nonlinear evolution of three-dimensional reconnection instabilities in a configuration where a guide field is present and many resonant surfaces are simultaneously excited in different locations of the simulation domain. The behavior of the system is different from the case when only an antiparallel magnetic field is present. We observe coalescence of magnetic islands and the formation of an anisotropic energy spectrum, which is more developed in the direction perpendicular to the local equilibrium magnetic field. The characteristics of the turbulence is different from magnetohydrodynamic turbulence with a uniform average magnetic field.

INTRODUCTION

The nonlinear evolution of reconnection instability in a current sheet can produce both coalescence of magnetic islands and development of turbulence. In two-dimensional situations it has been found that a chain of magnetic islands formed as a result of a tearing instability is subject to coalescence driven by the stretching of the most intense X points (Malara et al., 1992). Dahlburg and Einaudi (2002) studied three-dimensional instabilities in the case of an antiparallel equilibrium magnetic field, where only one resonant surface is present at the center of the current sheet. In this situation, coalescence is observed, but it is overcome by the growth of the $(0, 1)$ mode, the longest wavelength in the direction perpendicular to the plane where coalescence occurs. The final state is a 3D turbulent state and very little coalescence is observed. We show in this paper that when a guide field is present the nonlinear evolution is characterized by coalescence of 2D modes in the center of the current sheet and also by small scale structures produced by the energy cascade.

The presence of a background magnetic field has strong effects on the properties of the turbulence, which develops spectral anisotropy (Shebalin et al., 1983). For MHD turbulence with a uniform background magnetic field a spectral index $\gamma = -3/2$ has been predicted by Iroshnikov (1963) and Kraichnan (1965). However Goldreich and Sridhar (1997) taking into account spectral anisotropy, predicted a spectral index $\gamma = -5/3$. On the other hand, in the magnetotail and magnetopause turbulence, where the average magnetic field is not uniform, anisotropic energy spectra have been observed with spectral indexes up to $\beta = 3$ (Zimbardo, 2006). Anisotropy has been observed by many spacecraft in the solar wind turbulence (Horbury et al., 2005) and in various regions of the Earth's magnetosphere (Vörös et al., 2003). Experiments have also suggested the existence of spectral anisotropy in laboratory plasma devices (Zweben et al., 1979). Spectral anisotropy is also important for the transport of particles in turbulent plasmas, both in space and laboratory systems, since it produces anisotropy in the transport (Shalchi et al., 2004).

Besides the cases with a uniform average magnetic field, another context in which turbulence anisotropy is relevant is magnetic reconnection. In fact, when tearing-unstable modes grow to significant amplitudes, they couple nonlinearly producing a cascade to small scales (Malara et al., 1992, Onofri et al., 2004). Such a phenomenon is intrinsically anisotropic, since unstable modes, which give origin to the turbulent cascade, develop at wavevectors $\mathbf{k}$ locally perpendicular to the background magnetic field $\mathbf{B}_0$. Dahlburg et al. (2005) showed that, only if the rotation angle of the magnetic field across the current sheet is larger than 45°, a secondary instability of three-dimensional modes develops when the two-dimensional modes saturate. Here we present a simula-

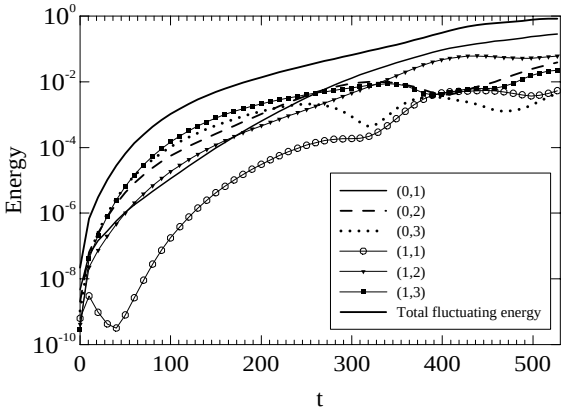

Figure 1: Energy of the most unstable modes.

tion of the magnetohydrodynamic (MHD) turbulence that is generated in this configuration when tearing modes grow and interact nonlinearly. We analyze the anisotropy properties of the turbulence generated by the nonlinear development of reconnection instability in a sheared magnetic field for large values of the rotation angle (greater than 45°). During the nonlinear evolution of the system, the interactions of the unstable modes produce the development of anisotropic MHD turbulence.

THE NUMERICAL MODEL

We solve numerically the incompressible, dissipative, magnetohydrodynamics (MHD) equations in dimensionless form:

$$\frac{\partial \mathbf{V}}{\partial t} + (\mathbf{V}\cdot\nabla)\mathbf{V} = -\nabla\left(P+\frac{B^2}{2}\right) + (\mathbf{B}\cdot\nabla)\mathbf{B} + \frac{1}{R_v}\nabla^2\mathbf{V} \quad (1)$$

$$\frac{\partial \mathbf{B}}{\partial t} = \nabla\times(\mathbf{V}\times\mathbf{B} + \frac{1}{R_M}\nabla\times\mathbf{B}) \quad (2)$$

$$\nabla\cdot\mathbf{V} = 0 \quad (3)$$

$$\nabla\cdot\mathbf{B} = 0 \quad (4)$$

where $\mathbf{V}$ and $\mathbf{B}$ are the velocity and magnetic field, respectively, P is the pressure and R_v and R_M are the kinetic and magnetic Reynolds numbers. Taking the divergence of Eq. (1) and using the condition (3) we obtain the equation for the total pressure:

$$\nabla^2 p = \nabla\cdot[(\mathbf{B}\cdot\nabla)\mathbf{B} - (\mathbf{V}\cdot\nabla)\mathbf{V}] \quad (5)$$

where $p = P + B^2/2$ is the total pressure.

We solve such equations in a three-dimensional Cartesian domain defined by: $-L_x \le x \le L_x$, $0 \le y \le 2\pi L_y$, $0 \le z \le 2\pi L_z$. We choose L_x as the unit length scale to non-dimensionalize the equations. In such a case, the numerical domain becomes: $D = [-1,+1]\times[0,2\pi l_y]\times[0,2\pi l_z]$, where $l_y = L_y/L_x$ and $l_z = L_z/L_x$ are the aspect ratios in the y and z directions, respectively.

We choose as unit measure for the magnetic field a typical value B_0, which allows us to define a characteristic value of the Alfvén velocity $v_A = B_0/\sqrt{4\pi\rho}$. The quantity ρ is the mass density, uniform everywhere. Hence, we express the velocity in terms of v_A and the time in terms of the typical Alfvén time: $\tau_A = L_x/v_A$. Finally, the pressure P is measured in units of ρv_A^2, while the definition of the Reynolds numbers, in terms of the kinematic viscosity ν and of the resistivity η, is: $R_v = v_A L_x/\nu$ and $R_M = v_A L_x/\eta$.

In the x direction we used the following boundary conditions:

$$B_x|_{x=\pm1} = 0 \quad (6)$$

$$\left.\frac{dB_y}{dx}\right|_{x=\pm1} = 0 \quad (7)$$

$$\left.\frac{dB_z}{dx}\right|_{x=\pm1} = 0 \quad (8)$$

$$\mathbf{V}|_{x=\pm1} = 0 \quad (9)$$

$$\left.\frac{dp}{dx}\right|_{x=\pm1} = 0 \quad (10)$$

which correspond to rigid conducting walls. Along the y and z directions we suppose to have periodic boundary conditions.

We set up the initial condition in such a way to have a plasma that is at rest, in the frame of reference of our computational domain, permeated by a background magnetic field sheared along the x direction, with a current sheet in the middle of the simulation domain. Therefore, we set, for the background quantities:

$$\mathbf{V}_0 = 0$$

$$\mathbf{B}_0 = B_{y0}\hat{y} + B_{z0}(x)\hat{z}$$

where B_{y0} is a constant value, which has been set to 0.5, while B_{z0} is given by:

$$B_{z0}(x) = \tanh\left(\frac{x}{a}\right) - \frac{x/a}{\cosh^2\left(\frac{1}{a}\right)} \quad (11)$$

This form for the magnetic field ensures that it is consistent with the boundary conditions, in particular the first derivatives along x of all the components of the magnetic field vanish at the boundaries.

The parameter a is a free parameter of our model, and represents the width of the magnetic field inhomogeneity. Under these conditions the initial total pressure is computed by solving numerically Eq. (5). In this configuration, we have a current sheet with a typical width a in the centre of the simulation domain. This is an equilibrium field in the ideal limit ($1/R_M = 0$). We perturb these equilibrium fields with three-dimensional divergenceless fluctuations of amplitude ϵ, which satisfy the boundary conditions. The periodicity in y and z imposes the following conditions on the wavenumbers:

$$k_y = m/l_y$$
$$k_z = n/l_z,$$

with m and n integer numbers. We explicitly solve the equations (1), (2) and (5) using a compact finite-difference scheme in the inhomogeneous direction (x) and a pseudo-spectral method in the periodic directions (y and z) (Onofri et al., 2004).

NUMERICAL RESULTS

A numerical simulation has been carried out with the following parameters:

$$N_x = 128, \quad N_y = 32, \quad N_z = 128$$

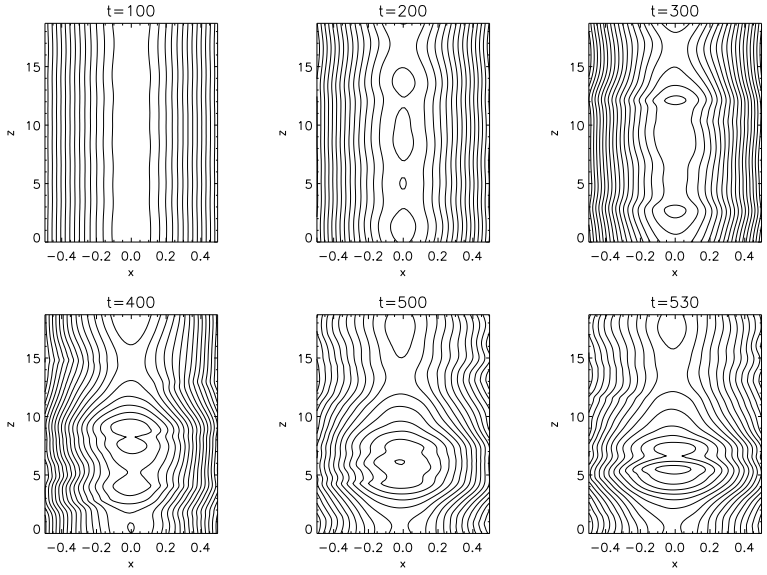

Figure 2: Magnetic field lines of the projected magnetic field $\mathbf{B}^{2D}(x,z) = B_x(x,0,z)\hat{x} + B_z(x,0,z)\hat{z}$ at different times.

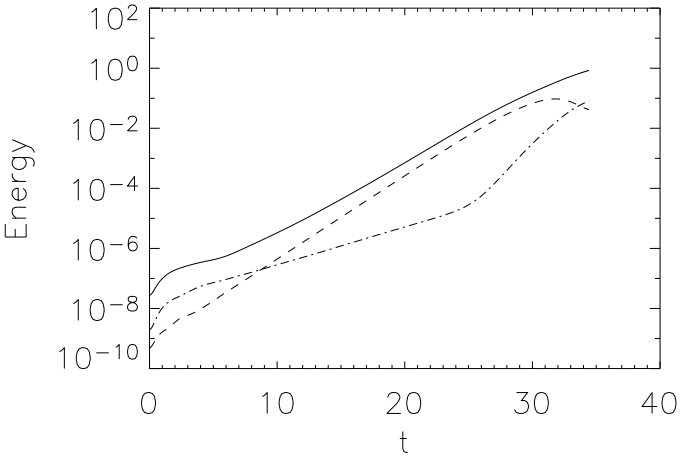

Figure 3: Time evolution of the energy of the modes $m = 0$, $n = 2$ (dashed line), $m = 1$, $n = 1$ (dotted-dashed line) and the total fluctuating energy (solid line).

$$R_M = 5000, \quad R_v = 5000$$
$$a = 0.1, \quad l_y = 1, \quad l_z = 3$$

The aspect ratios have been chosen taking into account that, according to the linear theory, the wave vector that corresponds to the maximum growth rate is $k \simeq 2$, so that $R_z = 3$ makes the $n \simeq 6$ modes the most unstable ones. This gives the possibility to observe energy transfer to both lower and higher wavenumbers. The width a of the current sheet has been chosen small enough to reduce stabilizing effects from the walls. We will show that the time evolution produces anisotropic spectra in the $k_y k_z$ plane, with an energy cascade mainly in the k_z direction (quasi-2D evolution). Hence a higher resolution is required in the z direction ($N_z >> N_y$). High resolution is also required along x, where small scales are produced by magnetic reconnection at the resonant surface locations. The equilibrium has been perturbed by exciting Fourier harmonics with $-4 < m < 4$ and $0 < n < 12$, which have resonant surfaces on both sides of the current sheet. The excited harmonics have wavelengths both shorter and longer than the most unstable mode, so nonlinear interactions can transfer energy in both directions. The x-integrated energy of the m, n Fourier mode is:

$$E^{tot}_{m,n}(t) = \int \frac{|V_{m,n}(t)|^2 + |B_{m,n}(t)|^2}{2} dx \qquad (12)$$

and the total fluctuation energy:

$$E_f(t) = \sum_{(m,n)\neq(0,0)} E_{m,n}(t)^{tot} \qquad (13)$$

In Fig. 1 the time evolution of the energy of the most unstable modes and of the total fluctuating energy is shown. At times $t > 200$ we observe a transfer of energy to smaller wavenumbers, which leads the $(0,1)$ mode to become the most energetic one. This corresponds in the physical space to a coalescence of magnetic islands along the z direction, and the growth of the $(0,1)$ mode can be seen as the formation of one magnetic island in the xz plane. To represent these phenomenon we consider the projection of the magnetic field onto the $y = 0$ plane: $\mathbf{B}^{2D}(x,z) = B_x(x,0,z)\hat{x} + B_z(x,0,z)\hat{z}$. In Fig. 2 the magnetic field lines of $\mathbf{B}^{2D}$ are shown at different times, the plots represent a narrow strip in the center of the domain. Magnetic reconnection and coalescence of magnetic islands are clearly visible.

Another simulation has been performed with a constant average magnetic field. This avoids the widening of the current sheet that would be produced by the small Reynolds numbers that are necessary for the numerical simulation. This is similar to what happens, on average, in current sheets that are found in astrophysical plasmas, like in the magnetotail. The growth of the unstable modes is faster and a larger spectrum is formed during the nonlinear evolution, with respect to the case where the equilibrium field is dissipated. In order to describe the whole spectrum, including the dissipative range, we have to use a high spatial resolution. The parameters used for this run are:

$$N_x = 128, \quad N_y = 512, \quad N_z = 1024$$
$$R_v = 1000 \quad R_M = 1000$$
$$a = 0.1 \quad l_y = 1, \quad l_z = 1,$$

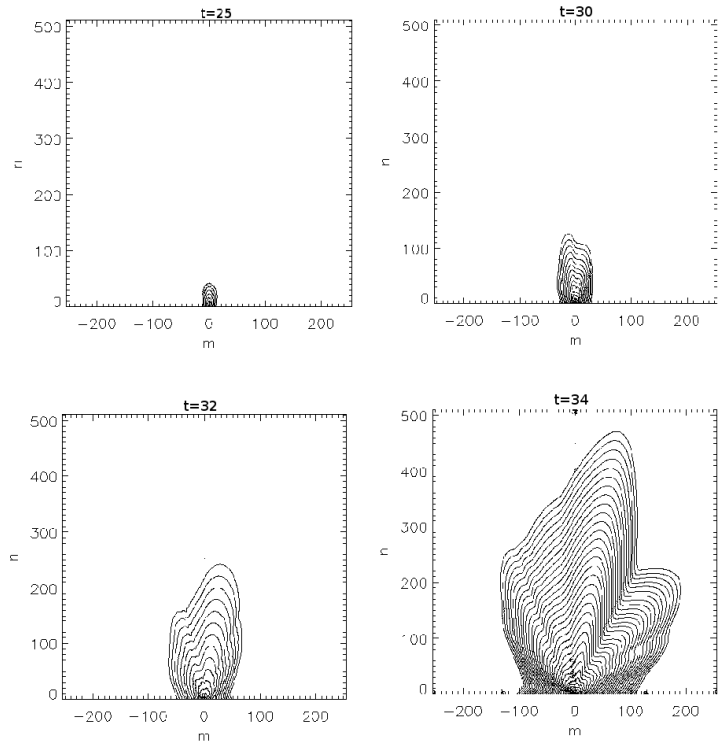

Figure 4: Contour plots of the total energy spectrum $\log(E^{tot}_{m,n})$ at different times. Time and $E^{tot}_{m,n}$ are normalized to τ_A and $\rho v_A^2 L_x$ respectively.

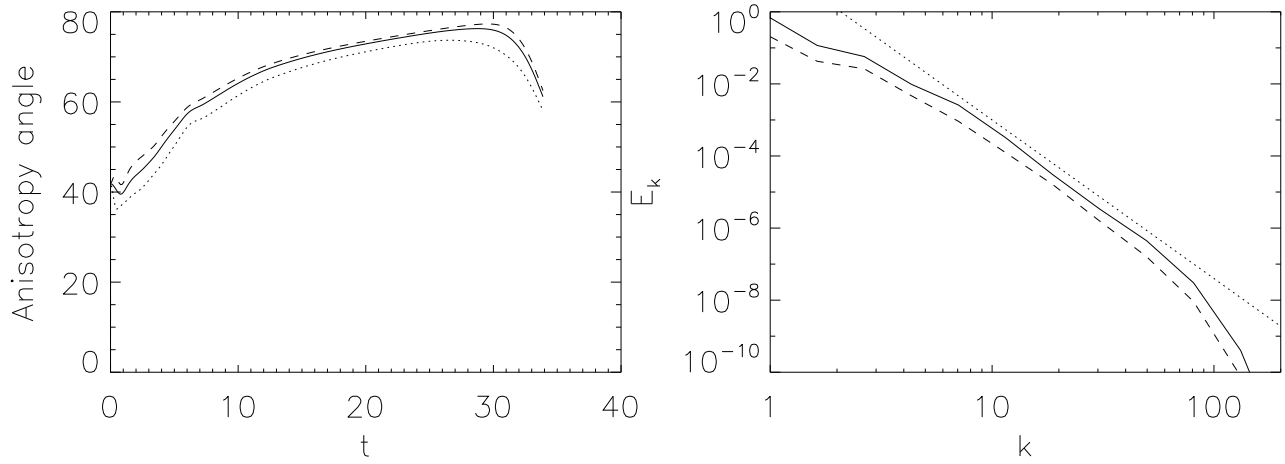

Figure 5: Anisotropy angle for kinetic energy (dotted line), magnetic energy (dashed line) and total energy (solid line). The angles are measured in degrees and time is normalized to τ_A

Figure 6: Spectrum of magnetic energy (solid line) and kinetic energy (dashed line) and $t = 34\tau_A$. The straight line corrsponds to a spectral index $\beta \simeq 4.3$. E_k is normalized to $\rho v_a^2 L_x^2$ and k to L_x^{-1}

To save computational time we also choose an aspect ratio for the simulation domain that does not allow the observation of coalescence.

In Fig. 3 the time evolution of $E^{tot}_{m,n}$ is shown for some of the most unstable modes, together with the total fluctuation energy. After an initial phase ($t < 6$), in which the unstable modes are formed, they grow exponentially. The $m = 0$, $n = 2$ mode is the most unstable, as predicted by the linear theory (Onofri et al., 2004). At later times ($t > 25$) nonlinear effects start to dominate the evolution and give origin to a transfer of energy among the different modes, producing an energy cascade to higher wavenumbers. At the same time we observe a change of slope of the $m = 1$, $n = 1$ mode, which corresponds to the secondary instability studied by Dahlburg et al.(2005).

Figure 4 shows the contour plots of the energy spectrum $\log(E^{tot}_{m,n})$ at times $t \geq 25$, when nonlinear interactions

among wavevectors dominate the spectrum evolution. The spectrum is anisotropic and it is developed mainly in the z direction, which is perpendicular to the equilibrium magnetic field in the center of the current sheet, where the most unstable modes grow. To give a measure of the $k_y k_z$ anisotropy we define an anisotropy angle:

$$\alpha = \tan^{-1} \sqrt{\frac{< k_z^2 >}{< k_y^2 >}}, \tag{14}$$

where $< k_y^2 >$ and $< k_z^2 >$ are defined as:

$$< k_z^2 >= \frac{\sum_{m,n} (n/l_z)^2 E_{m,n}}{\sum_{m,n} E_{m,n}} \tag{15}$$

$$< k_y^2 >= \frac{\sum_{m,n} (m/l_y)^2 E_{m,n}}{\sum_{m,n} E_{m,n}} \tag{16}$$

and $E_{m,n}$ can be either the magnetic energy, or the kinetic energy, or the total energy (Fig 5). An isotropic spectrum gives $\alpha = 45°$. The initial value of the anisotropy angle is around $42°$, then it increases during the simulation and it reaches a value of about $77°$ for the magnetic energy and $73°$ for the kinetic energy, indicating that wavevectors in the z direction prevail. The maximum values are attained before $t = 30$. In this phase most of the energy is concentrated in the modes with $k_y = 0$, which are the most linearly unstable. After $t \simeq 30$ the energy cascade becomes more efficient and the anisotropy angles start to decrease quickly. This can be seen in the two-dimensional spectrum (Fig. 4) as the appearance of different lobes at lower angles. The anisotropy that is observed in MHD turbulence with an average magnetic field is due to a larger rate of energy transfer in the direction perpendicular to the magnetic field, which may be interpreted in terms of the Alfvén effect.

In Fig. 6 we show the spectral energy density E_k, defined as:

$$E_k = \frac{e_k}{\Delta k}, \tag{17}$$

where e_k is the energy,integrated over the x coordinate, contained in the shell with wavenumbers between k and $k + \Delta k$ and the shells are logarithmically equally spaced. The kinetic energy is lower than the magnetic energy and the spectral index is $\beta \simeq 4.3$ for both spectra. This value of the spectral index is different from the values predicted for MHD turbulence with a uniform average magnetic field.

CONCLUSIONS

We studied the nonlinear evolution of three-dimensional instabilities in a configuration where a guide field is present and 3D perturbations are initially excited. Many resonant surfaces are simultaneously present in different locations and nonlinear interactions are also possible between unstable modes that correspond to different resonant surfaces. Energy transfer to both smaller and larger wavenumbers can take place due to our choice of the aspect ratios.

The final state of our simulation is a turbulent state, which is characterized by many spatial scales, with small structures produced by the direct energy cascade. On the contrary, the inverse energy transfer generates coalescence of magnetic islands, producing the growth of two-dimensional modes.

In another simulation we increased the resolution and kept constant in time the equilibrium magnetic field, which is not dissipated. In this case the aspect ratio does not allows the observation of coalescence, but the higher spatial resolution permits to analyze the anisotropy at small scales. We follow the development of the energy spectrum until energy is transported to the dissipative length scale. The spectral index is $\beta = 4.3$, which is different both from the Kolmogorov spectrum ($\beta = 5/3$) and from the Iroshnikov-Kraichnan spectrum ($\beta = 3/2$). The energy density spectrum is strongly anisotropic, developing mainly in one specific direction, which can be identified by the definition of an anisotropy angle. The spectrum grows mainly in the direction perpendicular to the equilibrium magnetic field.

The turbulence generated by magnetic reconnection is quite peculiar and it cannot be described by a standard homogeneous MHD turbulence, since both the spectral index and the anisotropy properties are different.

REFERENCES

Dahlburg, R. B., Einaudi, G., Physics Letters A **294**, 101, (2002).

Dahlburg, R. B., Klimchuk, J. A, Antiochos, S. H., Astrophys. J., **622**, 1191 (2005).

Horbury, T. S., Forman, M. A., Oughton, S., Plasma Phys. Control. Fusion, **47**, B703 (2005).

Iroshnikov, P., Soviet Astron., **7**, 566 (1963).

Kraichnan, R., Phys. Fluids, **8**, 1385 (1965).

Malara, F., Veltri, P., Carbone, V., Phys. Fluids B **4**, 3070 (1992).

Onofri, M., Primavera, L., Malara, F., Veltri, P., Phys. Plasmas, **11**, 4837 (2004).

Sahraoui, F., Belmont, G., Reseau, L., Cornilleau-Wehrlin, N., Pinçon, J.L., Balogh, A., Phys. Rev. Lett., **96**, 075002 (2006).

Shalchi, A., Schlickeiser, R., Astron. Astrophys., **420**, 821 (2004).

Shebalin, J. V., Matthaeus, W. H., Montgomery, D., J. Plasma Phys. **29** 525, (1983).

Zimbardo, G., Plasma Phys. Control. Fusion, **48**, B295 (2006).

Zweben, S., Menyuk, C., Taylor, R., Phys. Rev. Lett., **42**, 1270 (1979).